Optical response of localized excitons near surfaces of multilayer systems

1998 J. Phys.: Condens. Matter 10 79

(http://iopscience.iop.org/0953-8984/10/1/009)

J. Phys.: Condens. Matter **10** (1998) 79–88. Printed in the UK PII: S0953-8984(98)86427-8

Optical response of localized excitons near surfaces of multilayer systems

H A Coyotécatl† and G H Cocoletzi‡

† Facultad de Ciencias Físico-Matemáticas, Posgrado en Optoelectrónica, Universidad Autónoma de Puebla, Apartado Postal 1152, Puebla 72000, Mexico

‡ Instituto de Física, Universidad Autónoma de Puebla, Apartado Postal J-48, Puebla 72570, Mexico

Received 24 July 1997

Abstract. We study theoretically the effects of exciton bound states on the reflectivity of semiconductor superlattices and thin films. We consider direct gap semiconductors and assume extrinsic potentials near surfaces to model the exciton interactions. Using a multistep method and the 4×4 transfer matrix approach, we solve analytically the polariton exciton equations for s-polarized light. Results are presented for the $A_{n=1}$ excitonic transition of CdS and interpreted in terms of exciton bound states and Fabry–Pérot resonances of the transverse modes. We find that for the superlattice the reflectivity peaks of the high-energy bound states are notably enhanced as compared with the corresponding ones of the single isolated film.

1. Introduction

Optical properties of direct gap semiconductors, in the spectral region of excitonic transitions, have attracted the attention of recent publications [1–6]. The reflectivity of light is drastically modified by the presence of impurities near surfaces, in the so-called transition layer, due to the interaction of the excitons with the induced surface potential [6]. If no impurities are present in the semiconductor, the excitons are repelled into the bulk by the surface image potential [7, 8] and the non-escape condition [8, 9]. The presence of charge near the surface gives rise to extrinsic potentials that may attract or repel the excitons [1–6]. In addition, absorption processes may take place in the transition layer [1]. Consequently, close to the surface, polariton excitons may exhibit different behaviour compared to those in the bulk of the material [10]. Several theoretical models for semiconductor surfaces have been proposed since the primitive model of the 'dead layer' of excitons [7]. The 'dead' or 'inert' layer model assumes that an infinite abrupt potential is formed near the surface that repels the excitons. Besides this model, a linear continuous potential [11] has also been considered. However, the most realistic repulsive potential is the one with exponential variation [8, 12–14]. Using this exponential potential, studies have been made on the optical response of semiconductor surfaces and thin films [15], with satisfactory results for the reflectivity of semiconductor crystals [8]. It is worth noting that during the growth process, impurity atoms may be present to modify the properties of surfaces. For instance, band bending may be produced due to the presence of internal electric fields [16]. Recent publications have been devoted to studying optical properties of surfaces and films of semiconductors taking into account surface potentials with an attractive as well as a repulsive part [1–6]. The potential well formed in this way produces bound states of excitons

0953-8984/98/010079+10$19.50

which manifest themselves as broad peaks in the reflectivity spectra [17, 18]. Experimental observations on the effects of bound states on the optical response of semiconductor surfaces have been reported [17, 19–21].

In this report we present a multistep procedure [22] and the 4×4 transfer matrix approach to study the effects of exciton bound states on the optical response of semiconductor thin films and superlattices for s-polarized light. To see how the multistep approach works, we compared with previous results of semiconductor surfaces and films. We achieve good results when choosing steps of widths $d \leqslant 1$ Å. The report is presented as follows. In section 2 we explain the multistep method and develop the transfer matrix theory and in section 3 we discuss the numerical results and make conclusions.

2. Theory

Let us consider the superlattice constructed with layers and semiconductors and insulators: the interfaces are parallel to the xy-plane and the growth direction is along the z-axis. For the semiinfinite system we set the origin at the surface of the truncated superlattice. In the semiconductor layer we will consider different forms of the surface potentials. To construct the transfer matrix, we focus our attention on a single semiconductor layer of thickness d_s and apply a multistep approach. A schematic diagram is shown in figure 1.

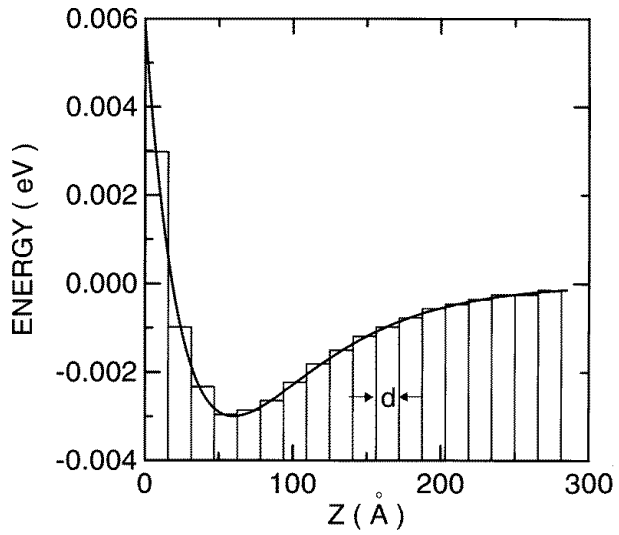

Figure 1. A schematic representation of the multistep method. The figure shows a typical Morse potential used for the calculations, with the steps and widths indicated.

To describe the polariton exciton, we deal with the equation of the excitonic polarization $\boldsymbol{P}$, which is obtained from the equation of motion of the exciton centre of mass and Maxwell equations. For s polarization we write $\boldsymbol{P} = (0, P(z)\,\mathrm{e}^{\mathrm{i}q_x x - \mathrm{i}\omega t}, 0)$ and the differential equation as [6]

$$\left[\frac{\partial^4}{\partial z^4} + \left(\varepsilon_0\frac{\omega^2}{c^2} - q_x^2\right)\frac{\partial^2}{\partial z^2}\right]P(z) + \left[\left(\varepsilon_0\frac{\omega^2}{c^2} - q_x^2\right)\Gamma^2(z) - \frac{\omega_p^2\omega^2 M}{c^2\hbar\omega_T} + \frac{\partial^2\Gamma^2(z)}{\partial z^2}\right]P(z) = 0 \qquad (1)$$

where

$$\Gamma^2(z) = \frac{M}{\hbar\omega_T}\left[\omega^2 - \omega_T^2(z) - \frac{\hbar\omega_T}{M}q_x^2 + \mathrm{i}\omega\nu(z)\right] \tag{2}$$

$$\nu(z) = \nu + h(z) \qquad h(z) = h_0\,\mathrm{e}^{(-z/a)} \qquad \omega_T(z) = \omega_T + 2U(z). \tag{3}$$

In these equations, q_x is the x-component of the wave vector, ω is the angular frequency, c is the speed of light in vacuum, $\hbar\omega_T$ is the energy of the excitonic transition, M is the mass of the exciton, ω_p is a measure of the oscillator strength, ε_0 is the dielectric constant of the background and ν is the damping parameter. The extrinsic surface potentials $U(z)$ that are studied in this report are the truncated Morse potential and the exponentially repulsive potential. Defining $|U_m|$ as the minimum value of $U(z)$ and z_m as the position of that mimimum, one can write, for the Morse potential, $U(z)$ as

$$U(z) = U_m|[\mathrm{e}^{-2(z-z_m)/a} - 2\,\mathrm{e}^{-(z-z_m)/a}] \qquad 0 < z < d_s. \tag{4}$$

To solve equation (1) rigorously, a series expansion may be used to take into account the dependence of z on Γ^2. An alternative procedure [22] consists in dividing the continuous potential in steps of constant potential, which in turn yields Γ^2 constant and allows the solution to be written as a superposition of exponentials in each step (see figure 1). The procedure is to construct the transfer matrix for a single step and then use boundary conditions to obtain the matrix for a layer. On the basis of this multistep method, for a step of width d_i $(=z_{i+1}-z_i)$ in the film, $P(z)$ is written in terms of the linear independent solutions $\mathrm{e}^{\pm\mathrm{i}q_n z}$, with $n = 1, 2$ and $z_i \leqslant z \leqslant z_{i+1}$. The solution for q_n (with $\mathrm{Im}\,q_n > 0$) is given as

$$q_n^2(\bar{z}_i) = \frac{1}{2}\left[\Gamma^2(\bar{z}_i) + \varepsilon_0\frac{\omega^2}{c^2} - q_x^2\right] \pm \frac{1}{2}\left[\left(\Gamma^2(\bar{z}_i) - \varepsilon_0\frac{\omega^2}{c^2} + q_x^2\right)^2 + \frac{4\omega^2\omega_p^2}{c^2 D}\right]^{1/2} \tag{5}$$

where $\bar{z}_i = (z_i + z_{i+1})/2$. Notice that the roots are determined by taking into account the potential $U(z)$, which enters in

$$\Gamma^2(\bar{z}_i) = [\omega^2 - \omega_T^2(\bar{z}_i) - Dq_x^2 + \mathrm{i}\omega\nu - \beta U(\bar{z}_i)]/D \qquad \beta = \frac{2\omega_T}{\hbar} \qquad D = \frac{\hbar\omega_T}{M}. \tag{6}$$

Since there are four propagating modes in each step, we consider four independent fields to construct the transfer matrix, namely, the tangential components of the electric field, E_y, and magnetic field, H_x, the excitonic polarization P and its derivative P'. Each field is expressed in terms of the amplitudes $E^{\pm}$ of the modes travelling to the right $(+)$ and to the left $(-)$. We write

$$E_y(z) = \sum_{n=1}^{2}(E_n^+\mathrm{e}^{\mathrm{i}q_n z} + E_n^-\,\mathrm{e}^{-\mathrm{i}q_n z}) \qquad H_x(z) = \frac{\mathrm{i}}{\omega}\frac{\partial E_y}{\partial z} \tag{7}$$

$$P(z) = \sum_{n=1}^{2} X_n(E_n^+\mathrm{e}^{\mathrm{i}q_n z} + E_n^-\,\mathrm{e}^{-\mathrm{i}q_n z}) \qquad P'(z) = \frac{\partial P(z)}{\partial z} \tag{8}$$

where

$$X_n = \frac{\omega_p^2}{4\pi D}\frac{1}{q_n^2 - \Gamma^2}. \tag{9}$$

In a matrix equation these fields may be written as

$$\begin{bmatrix} \boldsymbol{F} \\ \boldsymbol{P} \end{bmatrix}_z = G\begin{bmatrix} \boldsymbol{A}_1 \\ \boldsymbol{A}_2 \end{bmatrix}_z \tag{10}$$

where

$$\boldsymbol{F} = \begin{bmatrix} E_y \\ H_x \end{bmatrix} \qquad \boldsymbol{P} = \begin{bmatrix} P \\ P' \end{bmatrix} \qquad \boldsymbol{A}_n = \begin{bmatrix} E_n^+ \mathrm{e}^{\mathrm{i}q_n z} \\ E_n^- \mathrm{e}^{-\mathrm{i}q_n z} \end{bmatrix} \tag{11}$$

and

$$G = \begin{bmatrix} 1 & 1 & 1 & 1 \\ -Y_1 & Y_1 & -Y_2 & Y_2 \\ X_1 & X_1 & X_2 & X_2 \\ \mathrm{i}q_1 X_1 & -\mathrm{i}q_1 X_1 & \mathrm{i}q_2 X_2 & -\mathrm{i}q_2 X_2 \end{bmatrix} \tag{12}$$

with $Y_n = 1/Z_n$. Writing

$$\begin{bmatrix} \boldsymbol{A}_1 \\ \boldsymbol{A}_2 \end{bmatrix}_z = T(z - z') \begin{bmatrix} \boldsymbol{A}_1 \\ \boldsymbol{A}_2 \end{bmatrix}_{z'} \tag{13}$$

where $T(z) = \mathrm{diag}(\mathrm{e}^{\mathrm{i}q_1 z}, \mathrm{e}^{-\mathrm{i}q_1 z}, \mathrm{e}^{\mathrm{i}q_2 z}, \mathrm{e}^{-\mathrm{i}q_2 z})$ and diag(...) is a diagonal matrix constructor, we find that the fields at the right boundary z^R are related to the fields at the left boundary z^L ($z^R = z^L + d_i$) by

$$\begin{bmatrix} \boldsymbol{F} \\ \boldsymbol{P} \end{bmatrix}_{z^R} = M \begin{bmatrix} \boldsymbol{F} \\ \boldsymbol{P} \end{bmatrix}_{z^L} \tag{14}$$

where $M = GT(d)G^{-1}$ is a 4×4 matrix, with the elements having the form

$$\begin{aligned}
&M_{11} = [X_2 C_1 - X_1 C_2]/\Delta \qquad M_{12} = \mathrm{i}[-X_2 S_1/Y_1 + X_1 S_2/Y_2]/\Delta \\
&M_{13} = [C_2 - C_1]/\Delta \qquad M_{14} = [S_2/q_2 - S_1/q_1]/\Delta \\
&M_{21} = \mathrm{i}[-Y_1 X_2 S_1 + Y_2 X_1 S_2]/\Delta \qquad M_{22} = [X_2 C_1 - X_1 C_2]/\Delta \\
&M_{23} = \mathrm{i}[Y_1 S_1 - Y_2 S_2]/\Delta \qquad M_{24} = [C_2/\omega - C_1/\omega]/\Delta \\
&M_{31} = X_1 X_2 [C_1 - C_2]/\Delta \qquad M_{32} = \mathrm{i} X_1 X_2 [-S_1/Y_1 + S_2/Y_2]/\Delta \\
&M_{33} = [X_2 C_2 - X_1 C_1]/\Delta \qquad M_{34} = [-X_1 S_1/q_1 + X_2 S_2/q_2]/\Delta \\
&M_{41} = X_1 X_2 [-q_1 S_1 + q_2 S_2]/\Delta \qquad M_{42} = -\mathrm{i}\omega X_1 X_2 [C_1 - C_2]/\Delta \\
&M_{43} = [q_1 X_1 S_1 - q_2 X_2 S_2]/\Delta \qquad M_{44} = [-X_1 C_1 + X_2 C_2]/\Delta
\end{aligned}$$

where $S_i = \sin(q_i d)$, $C_1 = \cos(q_i d)$, $i = 1, 2$ and $\Delta = X_2 - X_1$.

The transfer matrix M is for the ith step, so we now involve the multistep procedure to obtain the total matrix of the semiconductor layer. We recall the fact that for each step in a layer there are four transverse modes, with two of them being additional propagating modes; furthermore, to achieve our goal, we shall use the following additional boundary conditions (ABCs) $P(z_i^+) = P(z_i^-)$ and $P'(z_i^+) = P'(z_i^-)$ together with Maxwell boundary conditions at the interface between the ith step and the $(i+1)$th step to construct the matrix. The final result can be written in terms of a product of matrices as $M_S = M_n M_{n-1} M_{n-2} \ldots M_1$.

After obtaining the matrix of a layer of thickness d_s, we invoke the ABCs at the free surfaces of the layer to reduce the 4×4 matrix to a 2×2, to be able to connect the fields with those of the insulating layer. The ABCs used for this purpose are written as [6] $[\alpha P + \partial_n P]_s = 0$. In this equation, α is a parameter and ∂_n is an outward normal derivative. When this ABC is applied, one can write [23]

$$\boldsymbol{F}(z_s^R) = N_s \boldsymbol{F}(z_s^L) \tag{15}$$

where N_s is now a 2×2 matrix, and z_s^R and z_s^L stand for the right and left boundaries of the layer. Applying Maxwell boundary conditions at the semiconductor layer–insulator layer interface, we obtain

$$\boldsymbol{F}(z_I^R) = M_t \boldsymbol{F}(z_s^L). \tag{16}$$

Here $M_t = M_I N_s$ is the total transfer matrix of a superlattice period $d = d_s + d_I$ and M_I is the 2×2 matrix of the insulator

$$M_I = \begin{pmatrix} \cos(q_I d_I) & -\mathrm{i}Y_I \sin(q_I d_I) \\ -\mathrm{i}Z_I \sin(q_I d_I) & \cos(q_I d_I) \end{pmatrix} \tag{17}$$

where $Z_I = q_I/\omega$ and $Y_I = 1/Z_I$.

For a superlattice with period d, we invoke Bloch's theorem to write

$$\boldsymbol{F}(z + d) = \mathrm{e}^{\mathrm{i}pd}\boldsymbol{F}(z) \tag{18}$$

with p being the one-dimensional Bloch wave vector. Combining these last two results, we may find the equation $\cos(pd) = \mathrm{Tr}(M_t)/2$ to determine p, where Tr denotes the trace of the matrix.

For the s-polarized light incident on the multifilm system, the reflectivity R_s in the surface impedance method is

$$R_s = \left|\frac{E_r}{E_i}\right|^2 = \left|\frac{Z_s(0)q_z + q_0}{Z_s(0)q_z - q_0}\right|^2 \tag{19}$$

where the surface impedance [24] is given by $Z_s(0) = E_y(0)/H_x(0)$. For the problem at hand

$$Z_s(0) = -\frac{M_{12}}{M_{11} - \mathrm{e}^{\mathrm{i}pd}} = -\frac{M_{22} - \mathrm{e}^{\mathrm{i}pd}}{M_{21}}. \tag{20}$$

3. Results and discussion

Numerical calculations are presented for superlattices of alternating layers of a semiconductor and an insulator, and an isolated semiconductor film. Our main purpose is to study the exciton bound states produced by attractive Morse potentials near surfaces, so for simplicity we consider vacuum as the insulator. To make the system precise, we consider the $A_{n=1}$ excitonic transition of CdS and study the optical response for s-polarized light. For this material, $\hbar\omega_T = 2.552\,72$ eV, $\hbar\omega_L = 2.554\,58$ eV, $M = 0.94\ m_0$, where m_0 is the rest mass of the electron. The parameter α appearing in the additional boundary condition (ABC) equations is taken to be large ($\rightarrow\infty$), so we only consider the Pekar ABC. The reason for this choice is that this ABC has been proved to give the best results when compared with experimental data [6].

In figure 2 we show the reflectivity R_s of light for a superlattice (curve a), an isolated film (curve b) and a single semiconductor surface (curve c). The energy eigenvalues $\hbar\omega_1 = 2.5499$ eV and $\hbar\omega_2 = 2.552\,37$ eV of the exciton bound states are taken from the literature as calculated for a single film [1]. Curves a and b exhibit similar structures below ω_T, where the shoulders are consequences of the bound states but shifted with respect to $\hbar\omega_1$ and $\hbar\omega_2$. Notice that the high-energy bound state shoulder is notably enhanced for the superlattice as compared with the corresponding one of the single isolated film. Moreover, we see that these two peaks are red shifted respect to those of the single surface. The fact that these two shoulders correspond to the bound states in the Morse potential has been already discussed in the literature for surfaces and thin films [1]. It has also been discussed that the maxima associated to bound states are shifted relative to the energy eigenvalues due to the interaction between the mechanical localized excitons and the electromagnetic fields in the medium (polaritonic effects). The additional structure of curves a and b is interpreted as Fabry–Pérot resonances of the transverse modes propagating in the semiconductor film. The resonances for the superlattice are notable enhanced when compared with R_s of the

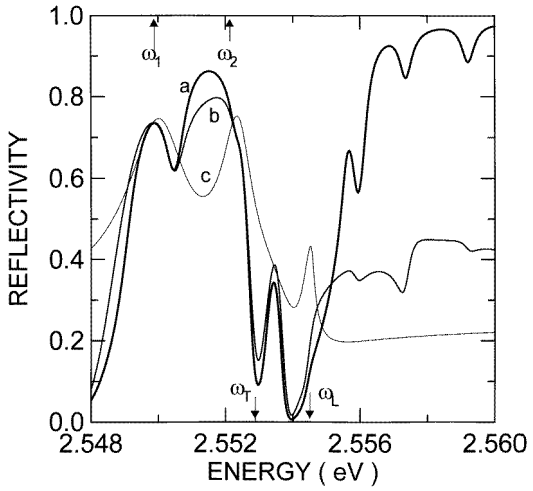

Figure 2. s-polarized light reflectivity R_s for a superlattice (a), a film (b) and a surface (c). Parameters correspond to the $A_{n=1}$ excitonic transition of CdS with $U_m = -5$ meV, $z_m = 60$ Å, $\overline{h}_0 = 2$ meV. The energies of the mechanical exciton bound states are indicated, as calculated for the single semiconductor film. $\overline{h}\omega_1 = 2.5499$ eV and $\overline{h}\omega_2 = 2.552\,37$ eV. ω_T and ω_L are indicated, and normal incidence of light is considered, $\theta = 0^\circ$. The effective thickness of the semiconductor film is $d_s = 620$ Å. The same value of d_s is used for the superlattice with an air gap of $d_I = 480$ Å.

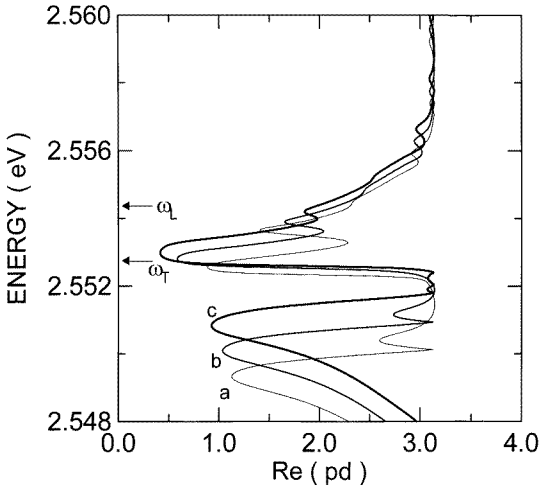

Figure 3. Real part of the dispersion relation ω against pd of the superlattice collective normal modes for three potentials. Curve a is for $U_m = -5$ meV, curve b is for $U_m = -4$ meV and curve c is for $U_m = -3$ meV. $z_m = 60$ Å, $\theta = 0^\circ$. The semiconductor layer has a thickness of $d_s = 620$ Å and the air gap of $d_I = 480$ Å.

single layer, as in the case of p-polarized light [23]. To test the multistep method, we have carried out comparisons of R_s with curves for single surfaces as well as for thin films, already reported in the literature [1], finding that the method works quite well when choosing widths of the step satisfying the conditions $d_i \leqslant 1$ Å.

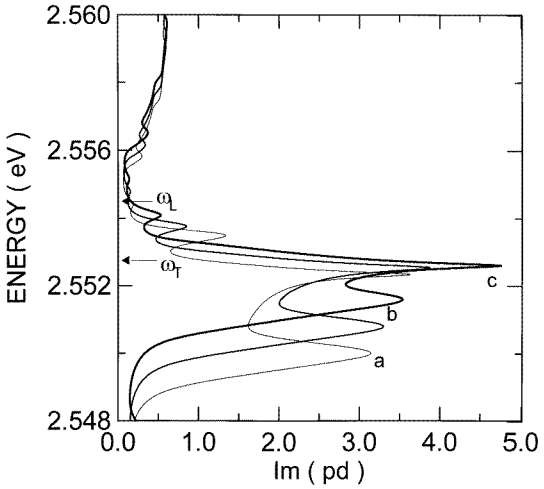

Figure 4. Imaginary part of the dispersion relation ω against pd of the collective normal modes for the same parameters as figure 3.

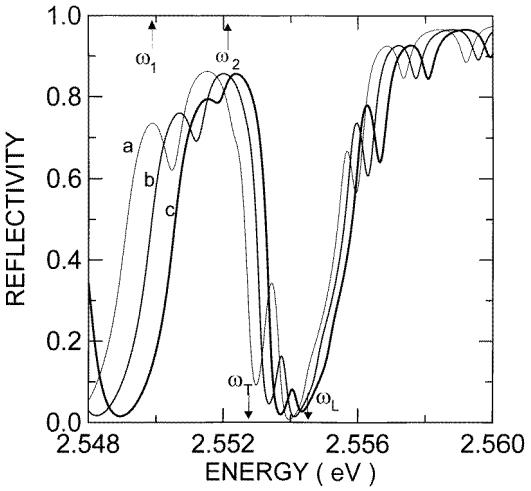

Figure 5. Reflectivity R_s of the semi-infinite superlattice for the same parameters as the dispersion relations shown in figures 3 and 4. Energies of the bound states are indicated for $U_m = -5$ meV, $\hbar\omega_1 = 2.5499$ eV and $\hbar\omega_2 = 2.552\,37$ eV.

In figures 3 and 4, we depict the dispersion relation of the collective normal modes for the superlattice ω against $\mathrm{Re}\,(pd)$ and ω against $\mathrm{Im}\,(pd)$, respectively, as functions of the minima of the potential well. Values of U_m are 5 for curve a, 4 for curve b and 3 for curve c. The structure of the exciton bound states is for energies below ω_T and is shown as maxima of the real part of Bloch's wave vector p, in the first Brillouin zone, and of Fabry–Pérot resonances in the layers above this energy. We notice that as the potential well becomes deeper the bound state energies as well as the resonances are red shifted. The imaginary parts of the dispersion relations presented in figure 4 show that the largest magnitude of $\mathrm{Im}\,(p)$ is for energies near the bound states when U_m takes the smallest value

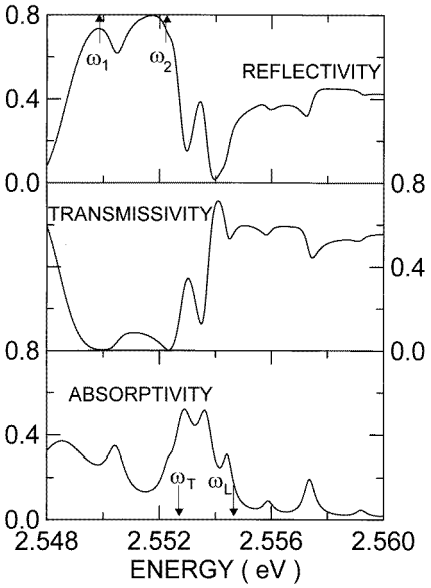

Figure 6. Reflectivity, transmissivity and absorptivity for a single isolated semiconductor film for a Morse potential and $U_m = -5$ meV and normal incidence of light. Bound state energies ω_1 and ω_2 are indicated. The film thickness is $d_s = 620$ Å.

and this magnitude decreases as U_m increases. The structure presented by the dispersion relations is manifested in the reflectivity curves as shown in figure 5, that is, whenever the real part of p presents a maximum, a maximum of R_s is also obtained. Moreover, the bound states shoulders are well defined and also red shifted as the potential well becomes deeper. Values of $\hbar\omega_1$ and $\hbar\omega_2$ are for $U_m = -5$ meV.

To complement the discussion on the exciton bound states, we display results for a single isolated semiconductor film. In figure 6, the reflectivity, transmissivity and absorptivity are presented for a film with effective thickness of 620 Å. The exciton bound states are located in the vicinity, but below ω_T and are manifested as shoulders of R_s. All other dips present in the curves are Fabry–Pérot resonances. In correspondence to the dips of the resonances, the transmissivity exhibits peaks and the absorption coefficient also displays structure.

In figure 7 are displayed the effects of different choices of surface potentials on the reflectivity for the same semiconductor film. We consider that the incident light shines on the left surface of the film with an angle of incidence of $\theta = 0^\circ$. Curve a is obtained with the Morse potential on the left surface and a pure repulsive potential on the right surface. The structure due to the two exciton bound states in the attractive potential well is clearly manifested as peaks, with a small blue shift induced by the imaginary part of the potential and polaritonic effects. Curve b accounts for pure repulsive potentials and only resonances are needed to explain the structure. The absence of any surface potential is considered in curve c where the structure is due to only Fabry–Pérot resonances. In this last case, the effective thickness is larger compared to the other two cases presented in the figure; furthermore, more resonances are allowed.

In conclusion, we have presented a study of excitons and exciton bound states in attractive surface potentials using a transfer matrix formalism and the multistep approach. We have considered superlatttices and isolated films of semiconductors to calculate the

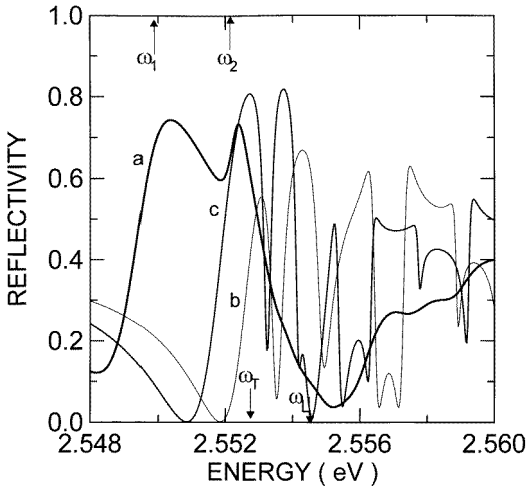

Figure 7. Reflectivity of a single film for different surface potentials. Curve a considers a Morse potential on the left surface with $U_m = -5$ meV and a repulsive potential on the right surface where $h_0 = 2$ meV. Curve b accounts for repulsive potentials on both surfaces, with a height of $h_0 = 2$ meV. In curve c no surface potential is included. ω_1 and ω_2 indicate the bound states in the Morse potentials with $U_m = -5$ meV. Normal incidence of light is considered.

optical response for s-polarized light. A comparison with the reflectivity of a single semiconductor surface obtained by solving the differential equations shows that the multistep method works quite well. The exciton bound states are clearly better manifested in both isolated films and superlattices, with an enhancement of R_s for the superlattice. From these results, we anticipate that exciton bound states are favoured to be observed experimentally.

Acknowledgments

Part of this work was performed while one of the authors (GHC) was visiting ICTP, Trieste, Italy. The financial support of CONACyT, Mexico, Project No 481100-5-5264E, is acknowledged.

References

[1] Pérez-Rodríguez F and Halevi P 1992 *Phys. Rev.* B **45** 11 854
[2] Halevi P and Pérez-Rodríguez F 1992 *Fiz. Nizk. Temp.* **18** 1135 (Engl. Transl. 1992 *Sov. J. Low Temp. Phys.* **18** 795)
[3] Pérez-Rodríguez F and Halevi P 1993 *Phys. Rev.* B **48** 2016
[4] Flores-Desirena B, Pérez-Rodríguez F and Halevi P 1994 *Phys. Rev.* B **50** 5404
[5] Pérez-Rodríguez F and Halevi P 1996 *Phys. Rev.* B **53** 10 086
[6] Halevi P (ed) 1992 *Spatial Dispersion in Solids and Plasmas (Electromagnetic Waves—Recent Developments in Research 1)* (Amsterdam: Elsevier) ch 6
[7] Hopfield J J and Thomas D G 1963 *Phys. Rev.* **132** 563
[8] Balslev I 1981 *Phys. Rev.* B **23** 3977
[9] D'Andrea A and Del Sole R 1982 *Phys. Rev.* B **25** 3714
[10] Kiselev V A 1978 *Fiz. Tverd. Tela* **20** 2173 (*Engl. Transl. 1978 Sov. Phys.–Solid State* **20** 1255)
[11] Sugakov V I and Khotyaintsev V N 1976 *Zh. Eksp. Teor. Fiz.* **70** 1566 (Engl. Transl. 1976 *Sov. Phys.–JETP* **43** 817)

[12] Skaistis E G and Khotyaintsev V N 1982 *Fiz. Tverd. Tela.* **24** 3648 (Engl. Transl. 1982 *Sov. Phys.–Solid State* **24** 2979)
[13] Ruppin R and Englman R 1984 *Phys. Rev. Lett.* **53** 1688
[14] Ruppin R 1984 *Phys. Rev.* B **29** 2232
[15] Halevi P, Hernández Cocoletzi G and Gaspar-Armenta J 1982 *Thin Solid Films* **89** 271
[16] Evangelisti F, Frova A and Patella F 1974 *Phys. Rev.* B **10** 4253
[17] Kiselev V A, Novikov B V, Utnasunov S S and Cherednichenko A E 1986 *Fiz. Tverd. Tela* **28** 2946 (Engl. Transl. 1996 *Sov. Phys.–Solid State* **28** 1655)
[18] Kiselev V A, Novikov B V, Batyrev A S, Ubushiev E A and Cherednichenko A E 1986 *Phys. Status Solidi* b **135** 597
[19] Zuev V A, Korbutyak D V, Kurik M V, Litovchenko V G, Rozhko A Kh and Skubneko P A 1977 *Pis. Zh. Eksp. Teor. Fiz.* **26** 455 (Engl. Transl. 1977 *JETP Lett.* **26** 327)
[20] Batyrev A S, Kiselev V A, Novikov B V and Cherednichenko A E 1984 *Pis. Zh. Eksp. Teor. Fiz.* **39** 436 (Engl. Transl. 1984 *JETP Lett.* **39** 528)
[21] Novikov B V, Ubushiev E A and Cherednichenko A E 1985 *Fiz. Tverd. Tela* **27** 1359 (Engl. Transl. 1985 *Sov. Phys.–Solid State* **27** 821)
[22] Kiselev V A 1982 *Solid State Commun.* **43** 471
[23] Cocoletzi G H and Mochán W L 1987 *Phys. Rev.* B **39** 8403
[24] Here we have used the + sign in front of Z_s to develop the algebra. However, it is more common to use the − sign for Z_s.